

CFD Calculation and Analysis of a 1.2NA Intake Duct

Hongxia Zhao*, Qingsong Zhu, Minjie Liu and Lin Zhou

Automotive Engineering Institute, Beijing Polytechnic, Beijing, 100000, China

*Corresponding author's e-mail: 103052@bpi.edu.cn

Abstract. In the development process of a 1.2NA engine air duct, to improve the overall power performance, we performed an optimization based on the original air duct, and the flow performance of the modified air duct was re-evaluated. This article applies AVL FIRE software to perform steady-state simulation analysis on the modified airway, obtaining the flow coefficient, roll ratio, velocity field, and pressure field distribution inside the cylinder under different fixed valve lifts. According to the AVL evaluation method, the average flow coefficient of the V1 intake duct of a certain 1.2NA engine is 0.3623, which is 4.8% lower than that of the V0 intake duct, and the flow coefficient is at a moderately low level. According to the FEV evaluation method, the average standard flow coefficient of the intake duct is 0.1008, which is 8.4% higher than that of the V0 duct, and the flow coefficient is at a moderate level. According to the AVL evaluation method, the average roll flow intensity of the V1 intake duct is 1.3953, which is 17.1% higher than that of the V0 intake duct, and the resulting roll flow intensity is at a moderate level. Airway tests are recommended to verify the calculation results.

Keywords: CFD; simulation analysis; gasoline engine; intake duct; rolling ratio

1 Introduction

In the early development process of a 1.2NA engine air duct, the overall power performance was optimized based on the original air duct, and the flow performance of the modified air duct was re-evaluated. This article applies AVL FIRE software to conduct steady-state simulation analysis on the modified airway, obtaining the flow coefficient, roll ratio, velocity field, and pressure field distribution inside the cylinder under different fixed valve lifts, and comparing them with the original airway^[1]. In the calculation of gasoline engine intake ports, the main parameters of concern are flow coefficient and tumble ratio. The flow coefficient directly determines the amount of charge in the cylinder, while the roll ratio has a significant impact on the formation, development, combustion diffusion speed, and stability of the mixture in the cylinder. Because increasing the flow coefficient will result in a decrease in the tumble ratio, and vice versa, it is often necessary to strike a compromise between the two^[2-4].

This calculation is a steady-state calculation, and the inlet and outlet boundary conditions adopt a pressure difference boundary. The inlet condition is total pressure, and the outlet condition is static pressure. The multidimensional numerical simulation calculation of the working process inside the engine cylinder satisfies the equations of

mass conservation, momentum conservation, and energy conservation, as well as the ideal gas state equation while selecting an appropriate turbulence model to close the equation system. The turbulence model used in this article is the k - ζ - f four equation model, which has a wide range of applications in the engineering field. For example, in the multidimensional numerical simulation of internal combustion engine cylinder flow, this model is used to describe the motion of turbulence in the cylinder^[5]. By simulating the flow inside the cylinder at different injection times, the influence of injection timing on combustion and emissions can be analyzed, providing a reference for the improvement and optimization of the injection system. It is a high-precision and high-stability turbulence model with wide application prospects and important engineering value. The k - ζ - f four equation model is a method of assuming and modeling the second-order related moment terms in the Reynolds equation, thereby enclosing the Reynolds equation system. Compared to the classical k - ϵ two equation model, this model has improved in terms of computational accuracy and stability^[6]. The k - ζ - f four equation model consists of the following four equations:

- The transport equation of turbulent kinetic energy k describes the variation of turbulent kinetic energy.
- The transport equation of turbulent dissipation rate ϵ , together with the k equation, describes the energy dissipation process of turbulence.
- The transport equation of the ζ equation: ζ is a variable related to the turbulence scale, which describes the variation of ζ .
- The transport equation of the f equation: f is a variable related to the turbulent vortex structure, which further describes the detailed characteristics of turbulence.

These four equations are interrelated and together form the complete system of the k - ζ - f four equation model. The characteristics and advantages of these four equations mainly include the following three aspects. High precision: The k - ζ - f four equation model can more accurately describe the complex characteristics of turbulence by introducing more variables and equations. High stability: Compared to other turbulence models, the k - ζ - f four equation model exhibits higher stability in the calculation process. Wide applicability: This model is suitable for various types of turbulent flows, including complex flow situations such as rotational flow and shear flow^[7-8].

2 Computational Model

2.1 Airway Test

Figure 1 shows the layout of the airway steady flow test bench, which consists of a cylinder head, a simulated cylinder, blades, a blade anemometer, a pressure gauge, a pressure regulator box, a blower, and a bypass. The test bench device operates in a suction mode. During operation, the blower sucks in air, and the air in the atmosphere flows in through the intake duct. It is then discharged into the atmosphere through simulated cylinder liners, pressure stabilizing boxes, orifice flow meters, etc. The U-shaped pressure gauge measures airway resistance, the orifice flowmeter measures airflow, the

rotating airflow drives the anemometer to rotate, the counter measures the number of revolutions, and the air volume is controlled by the regulating valve^[9].

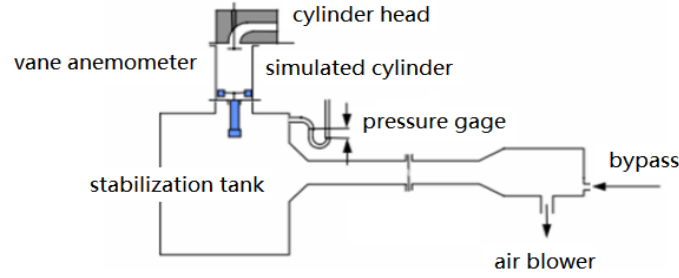


Fig. 1. Layout of airway test stand.

2.2 Calculation Grid

The computational model consists of an intake duct, intake valve, valve seat ring, combustion chamber top surface, and simulated cylinder liner. To ensure consistency between the computing environment and the experimental setup, we added a cubic stabilizing chamber at the inlet of the airway, simulating a cylinder liner length of 2.5 times the cylinder diameter. The lift point of the intake valve was calculated as 1 mm to 9 mm, and a calculation model was established every 1mm.

Using the preprocessing tool FAME Meshing of AVL-FIRE software for mesh generation, we set the basic mesh size to 2 mm, and some areas are further refined, including valve seats, intake valves, combustion chamber top surfaces, etc. The minimum mesh size is 0.125 mm. The total number of computational grids is approximately 1.2 million, as shown in Figure 2. The top view of the original airway V0 is shown in Figure 3, and the top view of the modified airway V1 is shown in Figure 4.

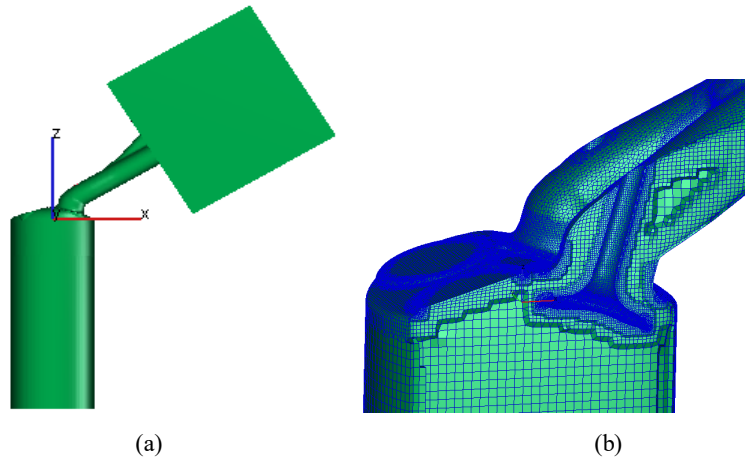


Fig. 2. Calculation grid.

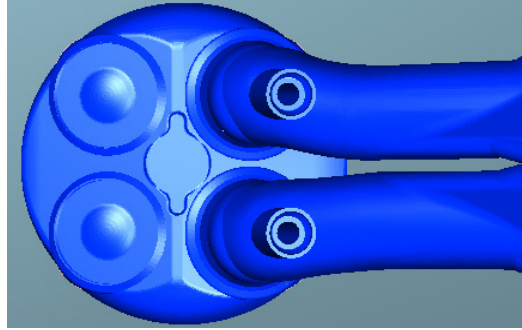


Fig. 3. Top view of a 1.2NA original airway V0.

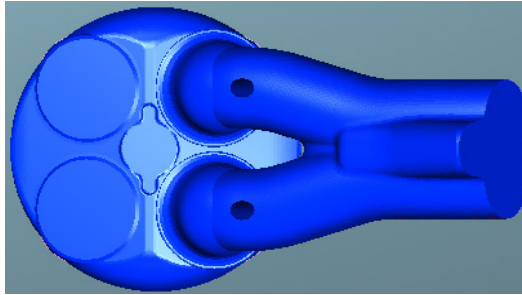


Fig. 4. Top view of a 1.2NA modified airway V1.

2.3 Evaluation Method

This article applies FIRE software to establish a calculation model based on the AVL airway test bench. The flow coefficient and roll ratio of the intake duct are calculated according to the AVL method, and the flow coefficient and roll ratio are evaluated and analyzed using the AVL method.

Flow Coefficient. According to AVL's evaluation method, the flow coefficient refers to the ratio of actual mass flow to theoretical mass flow. The theoretical mass flow rate is calculated based on the flow velocity and pressure drop over the valve seat area, assuming no flow loss. The specific formula is as follows:

$$\mu\sigma = \frac{m}{m_{th}} \quad (1)$$

$$m_{th} = z \frac{d_v^2 \pi}{4} \rho \sqrt{\frac{2\Delta p}{\rho}} \quad (2)$$

where m represents the actual mass flow rate; m_{th} represents the theoretical mass flow rate; $\frac{d_v^2 \pi}{4}$ indicates the area of the valve seat ring; d_v represents the minimum diameter of the valve seat ring; ρ represents gas density; Δp represents pressure drop.

The average flow coefficient is expressed as follows:

$$(\mu\sigma)_m = \frac{1}{\sqrt{\frac{1}{\pi} \int_0^\pi \left(\frac{c(\alpha)}{c_m}\right)^3 \frac{1}{(\mu\sigma)^2} d\alpha}} \quad (3)$$

When the valve lift is small, the AVL standard pressure difference is set to 6500 Pa, and when the valve lift is large, the AVL standard pressure difference is set to 2500 Pa.

Rolling Ratio. The rolling flow is a macroscopic large-scale vortex formed during the engine intake process. The rotational axis of rolling flow is perpendicular to the cylinder axis, and the definition of rolling flow ratio is shown in Figure 5. The rotational axis of rolling flow depends on the direction of the tangential airway.

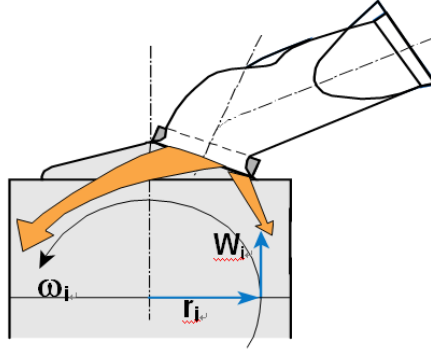


Fig. 5. Schematic diagram of rolling flow definition.

In steady-state calculations, it is generally believed that the line perpendicular to the cylinder axis and the airway section on the surface 0.5 times the cylinder head diameter is the rotational axis of the rolling flow. The rolling flow intensity calculated using FIRE software is based on the tangential component of the velocity on this plane (the velocity component parallel to the cylinder center axis). We assume that the average velocity of the piston is equal to the axial average velocity of the steady-state flow, and then, the calculation formula is as follows:

$$tumble\ ratio = \frac{n_D}{n} \quad (4)$$

$$c_m = \frac{sn}{30} = c_a = \frac{m}{\rho A_p} \quad (5)$$

$$n = \frac{30m}{\rho s A_p} \quad (6)$$

$$\frac{n_D}{n} = \frac{n_D \rho s A_p}{30m} \quad (7)$$

where c_m represents the average speed of the piston; s represents the engine stroke; n represents the engine speed; n_D represents the blade speed; c_a represents the average axial velocity of steady-state flow; m represents gas mass flow rate; ρ represents gas density; A_p represents the piston area.

Average tumble ratio:

$$\left(\frac{n_D}{n}\right)_m = \frac{1}{\pi} \int_0^\pi \frac{n_D}{n} \left(\frac{c(\alpha)}{c_m}\right)^2 d\alpha \quad (8)$$

In order to facilitate the evaluation of the engine flow coefficient between different cylinder diameters and valve seat diameters, the flow coefficient is standardized, and the standardized flow coefficient is represented as $\mu\sigma\beta$,

$$\beta = z \left(\frac{d_v}{D}\right)^2 \quad (9)$$

The simplified roll flow ratio is expressed as follows:

$$\left(\frac{n_D}{n}\right)_{red} = \frac{n_D}{n} \frac{D}{s} \quad (10)$$

where z represents the number of valves; D represents the cylinder diameter of the engine; s represents the engine stroke.

3 Boundary Conditions and Parameter Settings

3.1 Airway Test

This analysis is a steady-state calculation, assuming that the fluid is a compressible adiabatic flow process. Import and export use pressure difference boundary conditions. The inlet is the total pressure, and the outlet is the static pressure. To obtain accurate results in the experiment, we used different airway pressure differentials at different valve lifts, with a small valve lift pressure differential of 6500 Pa and a large valve lift airway pressure differential of 2500 Pa.

3.2 Input Parameters

The data that need to be input in the calculation settings file should be consistent with the experiment, as shown in Table 1.

Table 1. Input parameter table.

Name	Value/Unit
Cylinder diameter	69.70/mm
Stroke	79.00/mm
Minimum diameter of valve seat	26.00/mm
Number of valves	2/each

3.3 Solver Settings

For spatial discretization settings, extrapolate is chosen as the boundary value calculation method and Least Sq. Fit with higher calculation accuracy is chosen as the derivative calculation method; The coupling of speed and pressure adopts the SIMPLE algorithm; The turbulence model adopts $k-\zeta-f$; The momentum equation difference scheme adopts second-order accuracy with a softening factor of 0.5, the continuous equation difference scheme adopts center difference, and the others are upwind difference schemes; The wall treatment adopts a hybrid wall function, and the wall heat conduction adopts a standard wall function.

4 Result Analysis

4.1 Calculation Results 2D Data Analysis

Flow Coefficient and Roll Ratio of an Engine Intake Duct. According to the internal formula of FIRE, the flow coefficient and roll ratio under different valve lifts are obtained, as shown in Table 2. The average flow coefficient of the V1 intake duct of a certain 1.2NA engine is 0.3623, which is 4.8% lower than that of the V0 intake duct 0.3806; The average rolling flow intensity is 1.3953, which is 17.1% higher than the V0 airway 1.192.

Table 2. Flow coefficient and tumble ratio for fixed valve lift.

Intake Valve Lift hv (mm)	Flow Coefficient ($\mu\sigma$)	Rolling Ratio
1	0.1345	0.1001
2	0.2570	0.0654
3	0.3614	0.2306
4	0.4398	0.4683
5	0.4857	0.6850
6	0.5101	0.9304
7	0.5105	1.2975
8	0.5250	1.5038
9	0.5200	1.5484
Average value	0.3623	1.3953

According to the variation curves of flow coefficient and roll ratio, it can be seen that at low lift (1-6 mm), the flow coefficient of modified airway V1 is slightly lower than that of the original airway, while the roll ratio is comparable to that of the original airway; At high lift (6-9 mm), the flow coefficient is lower than that of the original airway, and the roll to roll ratio is significantly higher than that of the original airway. The modified airway V1 has good mixing ability for the mixture under atmospheric valve lift, which is shown in Figures 6 and 7.

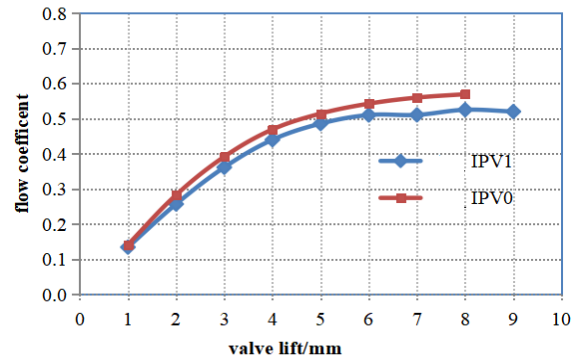


Fig. 6. 1.2NA airway flow coefficient variation curve.

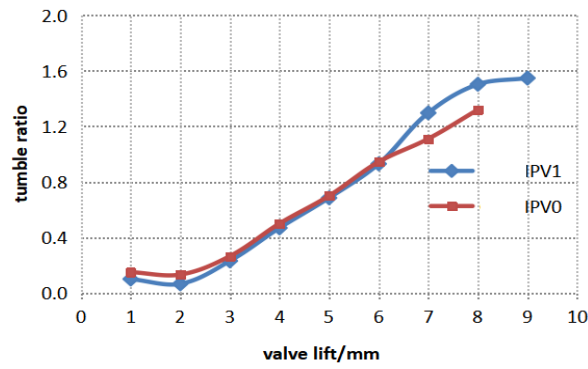


Fig. 7. 1.2NA airway roll flow ratio variation curve.

The flow coefficient and roll ratio curves of different models are shown in Figures 8 and 9. It can be seen from the figures that the flow coefficient of a certain V1 airway is at a medium-low level, and the roll ratio is at a medium level.

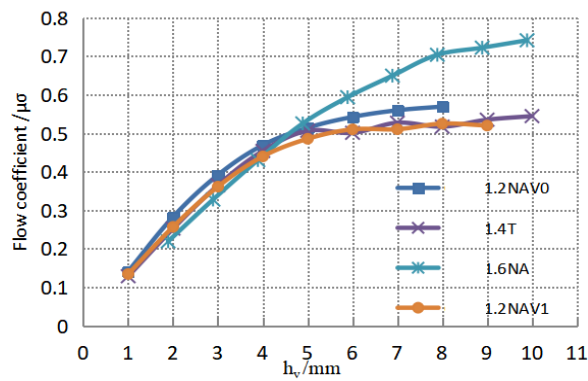


Fig. 8. Flow coefficient variation curves of different models.

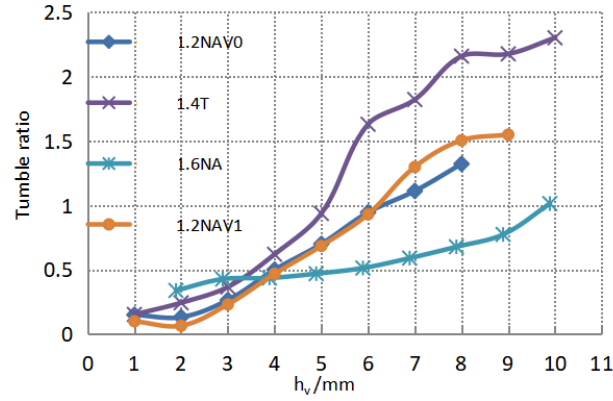


Fig. 9. Rolling ratio variation curves of different models.

Standardized Flow Coefficient and Simplified Tumble Ratio. According to the AVL evaluation method, the calculated flow coefficient is the ratio of the actual flow rate through the airway to the theoretical flow rate. It only represents the flow performance of the airway itself and cannot represent the flow performance of the airway after matching with the engine. Therefore, in the following analysis, the standardized flow coefficient and simplified roll ratio of parameters converted from the engine cylinder diameter and valve seat diameter are used.

Table 3. Standardized flow coefficient and simplified roll flow ratio for fixed valve lift.

Lift h_v (mm)	Standardized Flow Coefficient ($\mu\sigma\beta$)	Reduced Tumble Ratio
1	0.0374	0.0883
2	0.0715	0.0577
3	0.1006	0.2034
4	0.1224	0.4132
5	0.1352	0.6043
6	0.1420	0.8209
7	0.1421	1.1448
8	0.1461	1.3268
9	0.1447	1.3661
Average value	0.1008	1.2310

Table 3 shows the standard flow coefficient and simplified roll ratio values corresponding to each lift point. After matching the engine cylinder diameter, the average standard flow coefficient of this intake passage is 0.1008, which is 8.4% higher than that of V0 intake passage 0.093; The average value of rolling flow intensity is 1.2310, which is 17.1% higher than that of V0 airway 1.052.

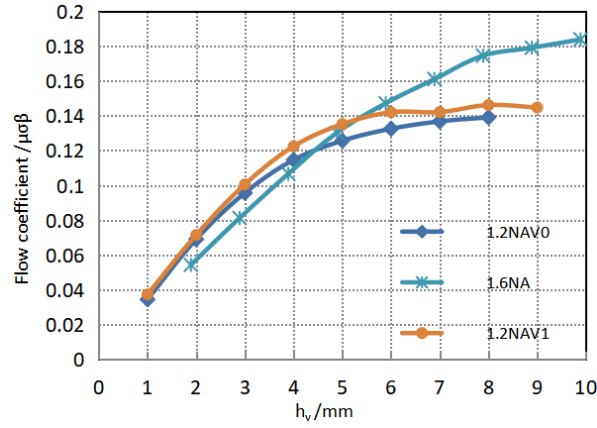


Fig. 10. Standardized flow coefficient variation curve.

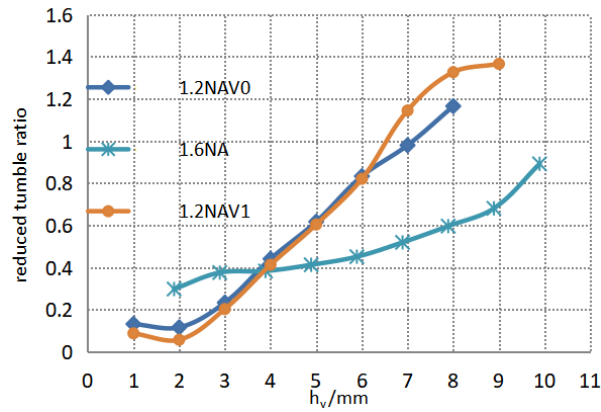


Fig. 11. Simplified roll flow ratio variation curve.

As shown in Figures 10 and 11, the standardized flow coefficient and simplified roll ratio of different models vary with valve lift. It can be seen that the standardized flow coefficient of a certain 1.2NA airway V1 is higher than that of the original airway at full valve lift because the inlet valve seat diameter of the modified airway V1 is 26 mm, which is higher than the original 24.63 mm; Due to the unchanged cylinder diameter and stroke, the simplified roll ratio and roll ratio are the same. Under atmospheric valve lift (6–9 mm), the modified airway V1 is higher than the original airway.

4.2 Slice Chart of Calculation Results

Figure 12 is a schematic diagram of the cross-sectional position of the calculation results in this article.

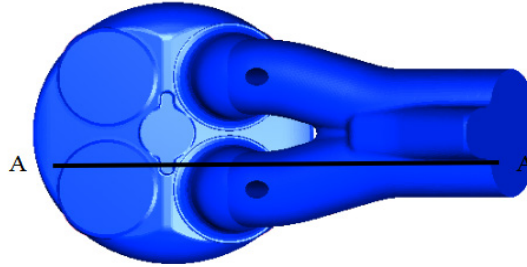


Fig. 12. Schematic diagram of A-A section.

The velocity field, pressure field, and turbulent energy field in Section A-A when the valve lift is 4 mm and 8 mm, respectively are shown in Figure 13-18.

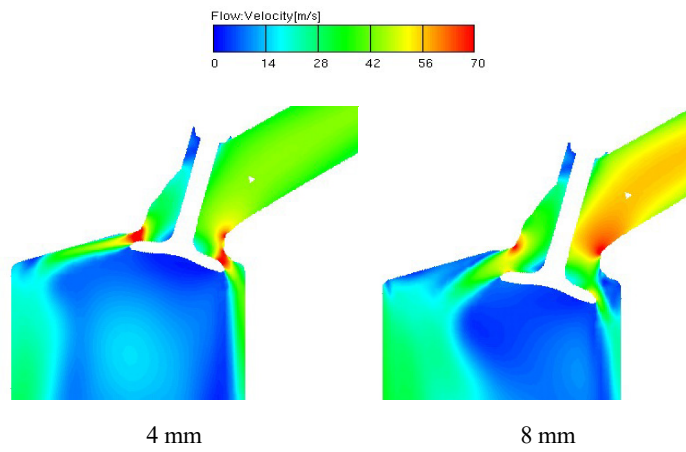


Fig. 13. Velocity field distribution_V0.

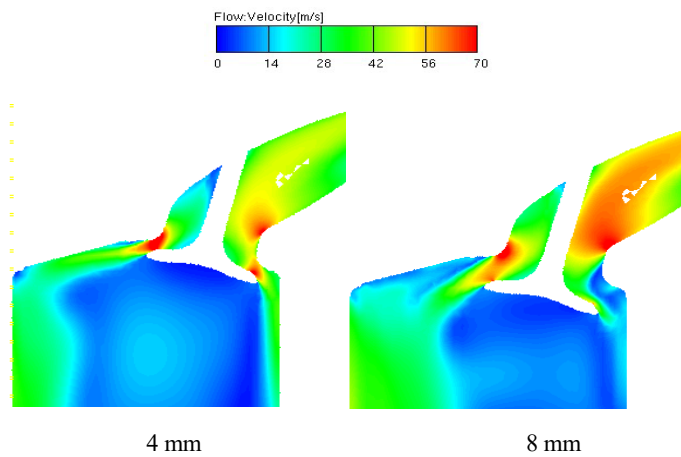


Fig. 14. Velocity field distribution_V1.

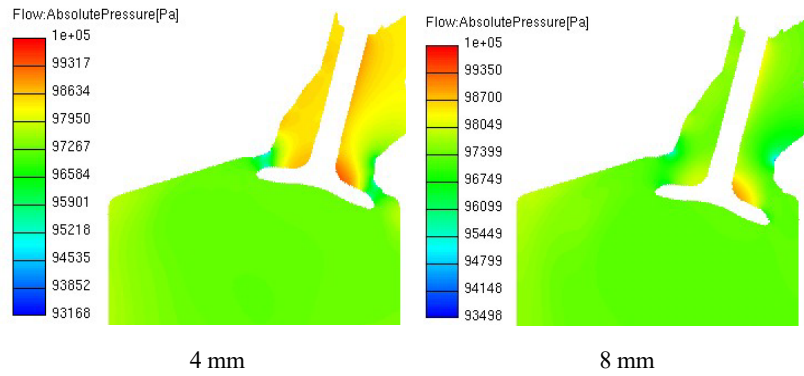


Fig. 15. Pressure field distribution_V0.

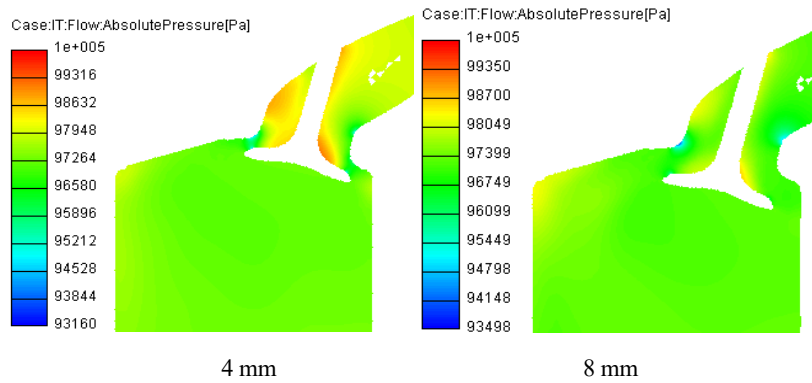


Fig. 16. Pressure field distribution_V1.

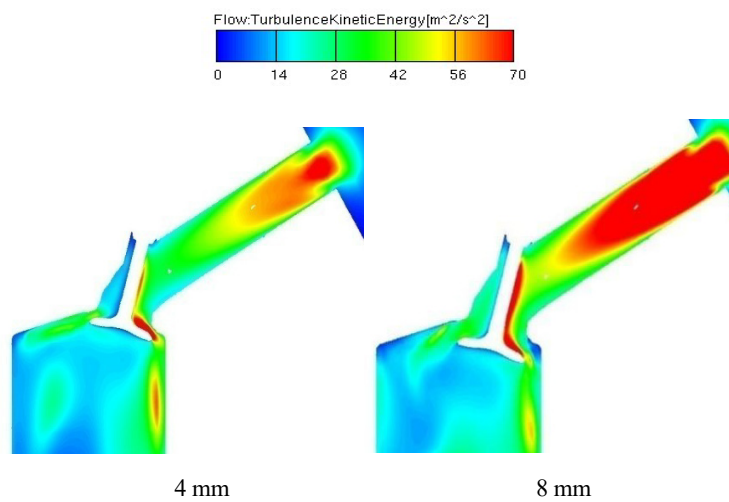


Fig. 17. Turbulent kinetic energy distribution_V0.

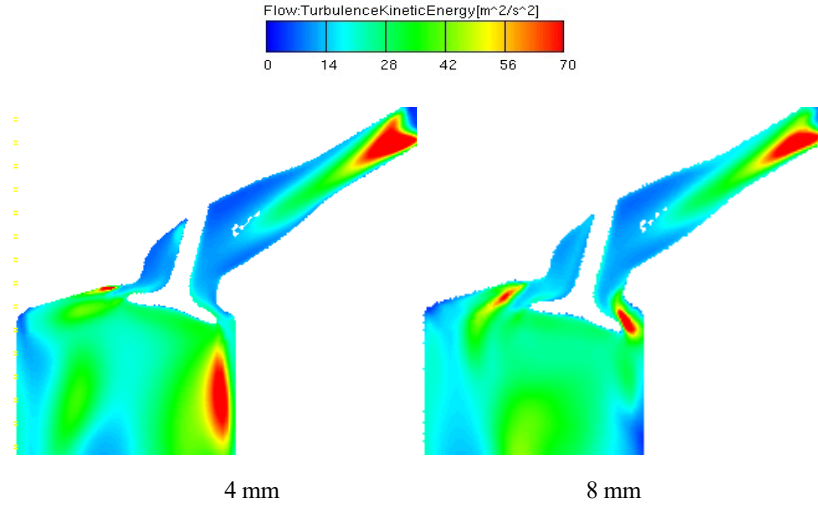


Fig. 18. Turbulent kinetic energy distribution_V1.

From Figures 13 and 14, it can be seen that at a valve lift of 4 mm, due to the throttling effect at the valve, the velocity at the intake valve throat is significantly higher than at a lift of 8 mm. From Figure 14, it can be seen that the velocity of the air entering the cylinder through the upper left intake surface of the valve is relatively high, which is conducive to the formation of rolling flow inside the cylinder. From Figure 17, it can be seen that the turbulence energy at point A in the original airway diagram is relatively large, and the energy loss of the airflow in the airway is relatively severe at this point; the turbulent energy loss of the modified airway V1 at the valve guide rod disappears.

5 Conclusion

By establishing a computational model for the intake duct and conducting CFD steady-state calculations, the conclusions are summarized as follows:

- According to the AVL evaluation method, the average flow coefficient of the V1 intake duct of a certain 1.2NA engine is 0.3623, which is 4.8% lower than that of the V0 intake duct 0.3806. The flow coefficient is at a moderately low level. It is recommended to conduct airway tests to verify the calculation results.
- According to the FEV evaluation method, the average standard flow coefficient of the intake duct is 0.1008, which is 8.4% higher than the V0 duct 0.093. The flow coefficient is at a moderate level.
- According to the AVL evaluation method, the average roll flow intensity of the V1 intake duct is 1.3953, which is 17.1% higher than that of the V0 intake duct 1.192. The rolling flow intensity formed is at a moderate level.

Airway tests are conducted to verify the calculation results.

Acknowledgments

This work was financially supported by the R&D Program of Beijing Municipal Education Commission (KM202310858005).

References

1. Wu Binyang, Jia Zhi, Li Zhen guo, et al. Different exhaust temperature management technologies for heavy-duty diesel engines with regard to thermal efficiency [J]. *Applied Thermal Engineering*, 2021, 186: 116495.
2. Vellandi V., Krishnasamy A. and Ramesh A. Transient emission characteristics of a light duty commercial vehicle powered by a low compression ratio diesel engine [C]. *SAE Technical Paper 2021-01-1181*, 2021.
3. Meng Zhongwei, Liu Zhentao and Liu Jinlong. Investigation of in-cylinder combustion deterioration of diesel engines in plateau regions [J]. *Fuel*, 2022, 324:124824.
4. Liu Jinlong, Li Yangyang and Zhang Chunhua. The effect of high altitude environment on diesel engine performance: Comparison of engine operations in Hangzhou, Kunming and Lhasa cities [J]. *Chemosphere*, 2022, 309: 136621.
5. Xiao Ge, Wang Yang, Zhang Heng, et al. Numerical study on the regeneration characteristics of catalytic diesel particulate filter based on real driving emissions in plateau environment [J]. *Fuel*, 2022, 321: 124020.
6. Piqueras P., Burke R., Sanchis E. J., et al. Fuel efficiency optimisation based on boosting control of the particulate filter active regeneration at high driving altitude [J]. *Fuel*, 2022, 319:123734.
7. Szedlmayer M. and Kweon C. M. Effect of altitude conditions on combustion and performance of a multi-cylinder turbocharged direct-injection diesel engine [C]. *SAE Technical Paper 2016-01-0742*.
8. Broatch A., Bermudez V., Serrano J. R., et al. Analysis of passenger car turbocharged diesel engines performance when tested at altitude and of the altitude simulator device used [J]. *Journal of Engineering for Gas Turbines and Power*, 2019, 141(8):1-9.
9. Wang Xin, Ge Yunshan, Yu Linxiao, et al. Effects of altitude on the thermal efficiency of a heavy-duty diesel engine [J]. *Energy*, 2013, 59: 543-548.